2mif

NASA TECHNICAL MEMORANDUM

NASA TM X-71589

NASA TM X-71589

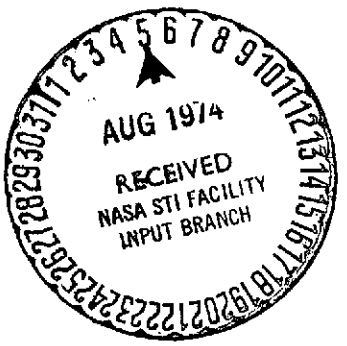

HIGH-TIP-SPEED FIBER COMPOSITE COMPRESSOR BLADES: VIBRATION AND STRENGTH ANALYSIS

by C. C. Chamis and J. E. Lynch
Lewis Research Center
Cleveland, Ohio 44135

TECHNICAL PAPER presented at
Second Conference on Fibrous Composites in Flight Vehicle Design
sponsored by the Air Force Flight Dynamics and Materials Laboratories
Dayton, Ohio, May 22-24, 1974

HIGH-TIP-SPEED FIBER COMPOSITE COMPRESSOR BLADES: VIBRATION AND STRENGTH ANALYSES

By

C. C. Chamis* and J. E. Lynch*

Lewis Research Center
National Aeronautics and
Space Administration
Cleveland, Ohio

E-8042

Abstract

An analytical procedure is described which couples composite mechanics computer codes with NASTRAN. This procedure was used to perform a detailed analysis of a high-tip-speed fiber composite compressor fan blade. The results indicate that the various vibration modes of this blade are highly coupled. Mechanical load ply stresses are well below the corresponding room temperature strengths. Lamination residual stresses are likely to cause transply cracks and interply delamination. Transply cracks and relaxation of root fixity decrease the vibrational frequencies whereas centrifugal stiffening increases them. Comparisons of results for various parameters are presented in tabular and graphical form.

* Aerospace Engineer

KEY WORDS: Computerized analysis, vibrational analysis, deflection analysis, stress/strength analysis, composite mechanics, NASTRAN, fiber composites, high-tip-speed, compressor-fan-blade

INTRODUCTION

NASA is currently conducting research programs on high-tip-speed transonic axial flow fan and compressor stage technology for tip speeds up to 1800 feet per second. Aerodynamic performance of the stages tested to date has been satisfactory, and mechanical problems have been minimal. However, to achieve the fan pressure ratio required for advanced engines, tip speeds on the order of 2200 feet per second are desired. Preliminary feasibility studies indicate that blades made from advanced fiber composites have the potential for attaining this level of tip speed. NASA has a research program under contract to design, fabricate, and test a research fan stage of advanced fiber composites with design tip speed of 2200 feet per second and a pressure ratio of 2.8.

Detailed analysis for deflections, vibration frequencies and modes, stresses and/or strains of such blades constitutes a major task. Therefore, it became necessary to develop an analysis capability for determining these variables.

This report does the following:

1. It describes an analytical procedure which couples NASTRAN with composite mechanics and which can be used for the analysis of high-tip-speed fiber composite compressor blades.

2. It assesses the adequacy of the selected design with respect to deflections, vibrations, and strength requirements.

COMPOSITE BLADE DESCRIPTION

A proposed design for the fan blades consists of HT-S graphite fibers in K601 polyimide matrix. The blade tip radius is about 16.3 inches. The rotor inlet aerodynamic hub-tip ratio is about 0.5. The root attachment chord is about 6.5 inches and the tip chord is about 7.8 inches. A photograph of a model of the blade is shown in Figure 1. This figure shows the blade as fabricated. The trimmed blade and the airfoil boundary are shown by the white stripes in the photograph. The blade has a nonlinear twist with an overall twist angle of about 31° from hub to tip. A view from the blade tip of the twist is shown in Figure 2.

The thickness percentages for ply orientations in the proposed blade design are: about 30 percent $\pm 40^{\circ}$ plies for the blade shell with no interspersed 0° plies, $\pm 20^{\circ}$ plies for transition, and about 70 percent 0° plies for the core. Near the blade tip, there are two surface plies $\pm 75^{\circ}$ to minimize cordiwise deflections. A computer representation of the ply contours is shown in Figure 3.

ANALYTICAL PROCEDURE - GENERAL DESCRIPTION

The analysis procedure consists of using NASTRAN in conjunction with composite mechanics embedded in pre- and postprocessors. The pre- and postprocessors are especially designed to automate the large amount of information needed to analyze fiber composite compressor blades via NASTRAN. The preprocessors are used to generate three types of information required as input for NASTRAN. Briefly, these types are:

1. Finite element representation, nodal coordinates, nodal thickness, and boundary conditions.

2. Nodal pressures and temperatures.

3. Anisotropic material properties generated from input constituent properties, fiber volume ratio, void ratio, ply orientation and ply contours.

The postprocessor is used to reduce NASTRAN output information into ply stresses and/or strains and the corresponding margins of safety. The NASTRAN output information, in general, consists of nodal displacements, element force resultants, element stresses and the corresponding principal stresses, and frequencies for various vibration modes. The overall blade untwist and uncambering are determined from nodal displacements at the tip.

For the analysis of the proposed blade, a triangular finite element representation is used. The element includes bending and membrane responses, centrifugal forces, and anisotropic material properties. This element is identified as CTRIA2 in the NASTRAN library of elements. A schematic of the finite element representation is shown in Figure 4. The finite element representation consists of 299 nodes and 531 elements. In the laminate analysis preprocessor, the number of nodes is 1131 because triangular elements with mid-nodes are used to account for thickness variations within the element. A schematic of the analytical procedure is shown in Figure 5. In this schematic, all the elements entering the blade analysis are identified.

VIBRATION AND STRESS ANALYSIS

Calculations were performed on the NASA-Langley Research Center CDC 6600 computer and on the NASA-Lewis Research Center Univac 1106 system. The NASTRAN program was used for the majority of these calculations, for both stress and normal mode frequency determinations.

Blade Geometry and NASTRAN Input Data Preparation

Descriptions of the blade airfoil surface contour, resulting from extensive aerodynamic flow analyses, were provided by the Design Contractor.[1] These descriptions are in the form of independent cartesian coordinates for each of twenty chordwise airfoil sections. Finite element nodal locations, which define the airfoil middle surface in a global cartesian coordinate system,

were prepared by a mesh generator computer program written for this purpose. This global coordinate system is shown in Figure 6, which also displays the blade twist in terms of tip, mid-span and root section orientations. Notice the relative thinness of the airfoil leading edge. Later it will be seen that this determines the detailed characteristics of the modal shapes. The finite element mesh, which utilizes 299 nodes and 531 thin-shell membrane and bending triangular elements of NASTRAN type CTRIA2, is shown in Figure 4.

The position of the gas flow path conical surface near the root is shown in Figure 1. Since the cone-shaped spacers located between blades, which define this flow surface, are supported entirely by the rotating disc and provide no significant reaction on the blade, no structural effect is considered along this line. Blade root attachment to the disc is idealized at the first line of nodes with a Y coordinate of 6.87 inches.

Resultant pressure loads, acting in the outward direction of the suction surface normal, were also provided by the Design Contractor. This loading, for the maximum design speed of 2200 feet-per-second at the tip, is shown in Figure 7.

Various boundary constraint conditions (end fixity) are applied at the idealized attachment radius as discussed in a later section. The actual three-dimensional nature of the dovetail attachment is not considered.

Property descriptions, in the NASTRAN MAT2 format for linear temperature - independent homogeneous anistropic materials, were prepared for the ply layup discussed previously. A uniform temperature of 300°F is used, which is an average over the small range of temperatures predicted for the airfoil.[1] The material axis orientation is 90° in magnitude for each element, which always has a chordwise local coordinate 1-2 axis orientation. Therefore, the material axis for the blade is oriented along the spanwise direction (Y coordinate, Figure 6).

Since NASTRAN utilizes a material description which ignores the details of ply layup, a separate material property generator program was utilized to prepare material properties using two different approximations. These will be referred to as the "equivalent bending stiffness" and "equivalent membrane stiffness" approximations.

Material Properties for Element Stiffness

The stress-strain temperature relationships accepted by NASTRAN Level 15.5 to generate the element stiffness are for a homogeneous material and are defined by

$$\begin{Bmatrix} \epsilon_{11} \\ \epsilon_{22} \\ \epsilon_{12} \end{Bmatrix} = \begin{bmatrix} G_{11} & G_{12} & G_{13} \\ G_{21} & G_{22} & G_{23} \\ G_{31} & G_{32} & G_{33} \end{bmatrix} \begin{Bmatrix} \sigma_{11} \\ \sigma_{22} \\ \sigma_{12} \end{Bmatrix} + \Delta T \begin{Bmatrix} \alpha_{11} \\ \alpha_{22} \\ \alpha_{12} \end{Bmatrix}$$

where ϵ denotes strain, σ stress, α coefficient of thermal expansion, ΔT temperature change above (below) some reference value and G the plane stress stress-strain relationships.

The blade is a laminated composite and not a homogeneous material. To use NASTRAN in the rigid format mode in this case, two approximations are necessary: (a) compute the various G's from the "equivalent membrane stiffness" or (b) compute the G's from the "equivalent bending stiffness". Both approximations are used to compute the G's and the results for deflections, stresses and frequencies are compared as will be described later.

The membrane and bending stiffnesses needed to compute the G's were generated by a multilayered fiber composite analysis computer code.[2] This computer code includes composite micromechanics, macromechanics, and laminate analysis. Using micromechanics, it is convenient to simulate gaps produced by residual stress transply cracks and interply delaminations. Transply cracks are simulated by voids in the present analysis.

The constituent material properties used and the unidirectional composite properties generated by the computer code, with and without voids, are summarized in Table 1. The properties used to simulate an interply delamination layer are summarized in Table 2.

The number of element material properties in NASTRAN Level 15.5 appears to be limited to about 100. In the finite element representation of the blade, 531 elements are used each with different material properties. To satisfy the element properties number limitation, the blade was divided into property regions as shown in Figure 8. All elements within each region are assigned the same material properties as the typical element, which was selected to represent the average of the region.

The material properties of the representative element are obtained by averaging the material properties computed at 6 element nodes, including 3 vertices and 3 midsides. This is done because the element has a variable thickness and because the number of plies and ply orientation is known only at these six nodes. Values of the G's for representative elements at a blade radius of 10.85 inches are shown in Table 3.

PARAMETERS INVESTIGATED

Several parameters are varied and the sensitivity of stress and frequency results is determined. The influences of root boundary conditions, rotational speed, and the material void fraction, to simulate transply cracks, are examined. The treatment of the material void fraction has been described in the Input Data Preparation Section.

Root Boundary Conditions

Three sets of single point nodal constraints at the root are utilized. The first set fixes all six (3-translational and 3-rotational) degrees of freedom (D.O.F.) at each root attachment node. The second set fixes only the three translational degrees of freedom at each node. The third set, which represents an intermediate condition, fixes several center nodes for all motions but allowes rotations at adjacent exterior nodes. Since the true dovetail structure, which consists of alternate layers of aluminum and composite materials, is not modeled, the relative accuracy of these three sets of design end conditions is to be determined by comparison with experimental measurements in the course of a continuing blade development program.

Rotational Speed and Centrifugal Stiffening

The centrifugal force field produces strains and differential stiffening effects. These speed-dependent differential stiffening effects are included in the vibration, deflection, and stress calculations. Since pressure loads also produce strains, differential stiffening effects due to these loads are also included at the maximum design speed for calculations of deflection, stress, and frequency. This is especially important in the determination of tip leading edge deflection and in the selection of the design setting angle and camber at the tip.

RESULTS AND DISCUSSION

Blade Tip Deflections

An assessment of the effects of the two different "equivalent stiffness properties" and voids/cracks on the blade response is obtained by examining the tip deflections.

Results of leading and trailing edge tip deflections for the cases examined are summarized in Table 4. The first six columns in Table 4 are NASTRAN nodal displacements. The last three columns denote blade-tip relative

displacements which are obtained from the first six by subtracting trailing edge values from the corresponding leading edge values. The significance of the results in the last three columns in Table 4 is as follows:

1. The radial deflection difference is a direct measure of the blade uniform/nonuniform radial growth.

2. The x and z coordinate deflection differences are a measure of the blade tip untwisting and uncambering.

Some observations from the results of Table 4 are:

1. "Bending equivalent stiffness" yields a more flexible blade response than the "membrane equivalent stiffness".

2. Transply crack simulation via void content reduces the blade stiffness.

3. Centrifugal stiffening has significant effects on the tip deflections. For the cases considered, centrifugal stiffening appears to compensate for the 20 percent void/crack effects.

4. Both "bending equivalent stiffness" and "membrane equivalent stiffness" yield nearly equal but nonuniform blade radial growth as measured by the difference in the radial leading and trailing edge tip deflections.

A computer plot of the undeformed and deformed blade tip positions at 100 percent design speed is shown in Figure 9. In Figure 9, the tip untwist angle and the leading edge uncamber angle are indicated. Note also the scale factor for determining the angles. Values measured for these changes are approximately: 1.5° for the untwist angle and 0.8° for the leading edge uncamber angle. A computer plot of the projected undeformed and deformed positions of the entire blade at 100 percent design speed is shown in Figure 10. As can be seen in Figures 9 and 10, the blade undergoes untwist, uncambering, and radial growth.

Vibration Frequencies and Modes

Results which appear in plotted form are based on the view direction indicated in Figure 6. The airfoil leading edge is shown at the left side on each view, which is of the pressure surface as projected onto a plane. Lines of minimum deflection are shown on each deformed shape plot. Dashed lines describe the original undeformed blade position. Although not displayed here, nodal deflection vector projections were utilized as aids in providing the minimum displacement locations, indicated by the bold solid lines.

Figures 11 through 16 depict the first six normal mode shapes for zero rotational speed, three translational D.O.F. fixed at each root node, and the "equivalent membrane stiffness" material approximation with 20 percent void/crack content. Figure 17 displays the changes in frequency as a function of speed for the same material. Variations in frequency for the first four modes are tabulated as a function of root fixation, material approximation and void/crack content in Table 5.

An examination of Figures 11 through 16 suggests that, in general, the mode shapes for this tapered twisted airfoil shell are strongly coupled motions which cannot be discussed in terms of classical beam or plate mode shapes. The exceptions are Modes 1 and to some extent 2 in Figures 11 and 12, respectively. These modes are predominantly first spanwise bending and torsion, respectively. It is particularly evident that the thin leading edge undergoes large deflections in all the vibrational modes.

A similar departure from the classical beam or plate results is seen in Figure 17. All modes have a noticeable frequency vs. speed dependence, including those which contain torsional motions. However, modes numbered 2 and 5 show only small changes with speed. Mode 2 has already been identified as a predominantly torsional motion. Mode 5 is predominantly a chordwise bending mode.

Table 5 indicates differences between frequencies of approximately 7 to 12 percent at zero speed for the two end conditions, which are equivalent to complete and zero rotational nodal constraint. Notice that all frequencies decrease for the latter condition. No positive statement can be made yet on the proper choice of end conditions for design purposes, although preliminary results from vibrational measurements favor the softer rotational end condition.

Table 5 highlights the difficulty in using current NASTRAN elements in the rigid format mode for laminate analysis. The spread of 10 percent in frequencies for the three higher modes as computed from the two different material equivalent approximations is quite significant when compared with the present design allowable of 5 percent spread for metal blades.

The results for crack (void) effects in Table 5 suggest that complete control and knowledge of void content and residual stress cracking is important if vibrational frequencies are to be predicted for composite blades with reasonable confidence.

Another observation that can be made, based on Figure 17, is the following. If the assumptions of 3 D.O.F. root fixation, "equivalent membrane stiffness", and 20 percent void content for residual stress transply crack simulation correctly represent the blade, then there is a possibility for coincidence of the first mode frequency with the twice per revolution excitation near 90 percent design speed.

Average Composite Stresses

Average composite extreme fiber stresses as determined by NASTRAN and the ply stresses are presented. Stresses are displayed for "bending equivalent stiffness" with no cracks, and "membrane equivalent stiffness" with cracks and two delamination layers. Stresses are also for blade temperatures at 100 percent design speed; residual stresses due to cure temperature are presented for the "bending equivalent stiffness."

NASTRAN output stresses consist of element centroidal stresses at the top and bottom of the element in the element local coordinates and the corresponding principal stresses in the same coordinates.

A contour plot of the radial (span-wise) stress at the pressure surface of the blade for the "equivalent bending stiffness" is shown in Figure 18 for two levels of stresses. As shown in Figure 18, the maximum average composite radial stress is concentrated in a relatively small region at the center of the blade (10.85 inches radius). Stress values at selected locations on the blade surface, points A, B, C, and D, Figure 18, are given in Table 6. These points were selected because the maximum radial stress occurs at point A, the maximum tangential stress at point B, and the maximum shear stress at point D. Point C was selected to show the stress variation in the maximum stress region.

Stress values computed from the "equivalent membrane stiffness" are summarized in Table 7. In Table 7, stress values are given for the following cases:

1. No cracks and no centrifugal stiffening.

2. Cracks with delamination but no centrifugal stiffening.

3. Cracks with two delamination layers and centrifugal stiffening.

Note for these cases that the stresses are computed at points A, B, D, and E. Note also that the maximum shear stress occurs at point E, Figure 18, as compared with point D for the case computed from "equivalent bending stiffness."

Comparing corresponding stress values from Tables 6 and 7 for points A, B, and D it is seen that the stresses computed from the "equivalent bending stiffness" exceed those computed using the "equivalent membrane stiffness" by more than ten percent.

Ply Stresses and Comparisons with Unifirectional Composite Fracture Stresses

The ply stresses were calculated using a multilayered fiber composite computer code.[2] The inputs for these calculations consistof the ply lay-up

configuration, the surface stresses from NASTRAN, constituent properties, and fiber and void volume ratios. (See analysis procedure schematic Figure 5.) Ply stresses are displayed for each representative material region in Figure 8.

Ranges of ply stresses at points A (point of maximum stress) and E, Figure 18, are summarized in Table 8 for various conditions. These conditions include mechanical load only, mechanical load with thermal load, thermal load only for residual stresses, and mechanical load only with centrifugal stiffening. The room temperature fracture stresses of the unidirectional composite are entered in the last line of Table 8 for comparison purposes.

The following observations pertain to the data in Table 8:

1. Some plies are subject to compressive stresses along the fiber direction. This can be detrimental at elevated temperatures if the selected matrix loses stiffness rapidly.

2. For the case of "mechanical load only" and no voids, the maximum stresses transverse to the fiber direction do not exceed the corresponding strength of the unidirectional composite.

3. For the cases of "thermal load only" and "mechanical and thermal loads" the transverse stress is greater than three times the corresponding unidirectional composite strength in some plies.

4. The maximum longitudinal tensile stress is about 40 percent of the corresponding unidirectional composite strength.

5. The maximum intralaminar shear stress is about 60 percent of the corresponding unidirectional composite strength.

6. The interply strain causing delamination is close to the corresponding estimated critical value.

The conclusions from the above observations are:

1. Lamination residual stresses are likely to produce transply cracks and intraply delaminations.

2. The unidirectional composite longitudinal compressive strength could be important in composite blades operating at elevated temperatures.

3. The maximum longitudinal tensile and intralaminar shear stresses are about 40 and 60 percent respectively below the corresponding room temperature unidirectional composite strengths.

4. Stress analysis of the blades should include the various combinations of the expected load conditions. Otherwise, the computed ply stresses will lead to misleading conclusions.

It is noted in passing that the maximum ply stresses are at a leading edge element in the transition region from airfoil to straight root section. This element is defined by nodes 32, 31, and 16 in Figure 4. However, these stresses are highly localized and decrease very rapidly to considerably smaller values at point A, Figure 18. Therefore, any damage caused by these high ply stresses will be confined to a very small area in the transition region.

SUMMARY OF RESULTS

The results of an investigation to develop a capability for analyzing high-tip-speed composite blades and for using this approach in a blade design are summarized below:

1. An analytical capability has been structured to couple composite mechanics with NASTRAN for the detailed vibration, deflection, and stress analysis of fiber composite compressor blades.

2. Applying this analytical capability to the 2200 feet per second tip-speed fiber composite blade has shown that:

   a. The various blade modes are highly coupled.

   b. The blade undergoes significant leading edge and tip vibrational motions and steady state tip deflections.

   c. Root fixity relaxation and transply cracks reduce the blade frequencies.

   d. Centrifugal stiffening provides significant blade stiffening at 100 percent design speed.

   e. Frequencies calculated using alternately "equivalent bending stiffness" and "equivalent membrane stiffness" may differ by about 10 percent.

   f. The high average composite stress is concentrated in a small region at the center of the blade near the gas flow boundary.

   g. Ply stress due to mechanical blade loads only are well below the corresponding room temperature strengths.

   h. Transverse ply lamination residual stresses exceed the corresponding ply strength in most of the blade and are likely to cause transply cracking. Lamination residual stresses are also likely to cause some interply delamination.

REFERENCES

1. Ultra High Speed Axial Flow Fan Stage, NASA Contract No. NAS3-15335 with Pratt and Whitney Aircraft, East Hartford, Connecticut.

2. Chamis, C. C.: Computer Code for the Analysis of Multilayered Fiber Composites - Users Manual. NASA TN D-7013, 1971.

TABLE 1.
CONSTITUENTS AND COMPOSITE ELASTIC AND THERMAL PROPERTIES

PROPERTY & UNITS	HT-S FIBER	K601 POLYIMIDE	UNIDIRECTIONAL COMPOSITE 0-VOIDS	UNIDIRECTIONAL COMPOSITE 20% VOIDS
*ELASTIC MODULUS (10^6 PSI)				
E_{11}	32.0	0.50	18.4	14.8
E_{22}	2.5	.50	1.43	1.23
E_{33}	2.5	.50	1.43	1.23
SHEAR MODULUS (10^6 PSI)				
G_{12}	1.5	.18	.70	.56
G_{13}	1.5	.18	.70	.56
G_{23}	1.0	.18	.46	.37
POISSON'S RATIO				
ν_{12}	.20	.41	.26	.24
ν_{13}	.20	.41	.26	.24
ν_{23}	.25	.41	.54	.53
COEFF OF THERMAL EXPANSION (10^{-6} IN./IN./^{0}F				
α_{11}	-.56	57.8	.12	.12
α_{22}	5.6	57.8	26.1	25.6
α_{33}	5.6	57.8	26.1	25.6

*SUBSCRIPTS 123 DENOTE MATERIAL AXES WITH 1 ALONG THE FIBER. CS-70181

TABLE 2.
ELASTIC AND THERMAL PROPERTIES OF DELAMINATED LAYER

PROPERTY	VALUE
ELASTIC MODULI (PSI)	
E_{11}	200
E_{22}	431
E_{13}	431
SHEAR MODULI (PSI)	
G_{12}	75
G_{13}	75
G_{23}	73
POISSON'S RATIOS	
ν_{12}	.27
ν_{13}	.27
ν_{23}	.58
COEFFS OF THERMAL EXPANSION, 10^{-6} IN./IN./^{0}F	
α_{11}	54.0
α_{22}	54.0
α_{33}	54.0

FOR SUBSCRIPT NOTATION SEE TABLE 1. CS-70178

TABLE 3.
REPRESENTATIVE ELEMENT PROPERTIES AT RADIUS 10.85 IN.

PROPERTY	LEADING EDGE			MID-SECTION			TRAILING EDGE		
	BENDING "0" VOIDS	MEMBRANE		BENDING "0" VOIDS	MEMBRANE		BENDING "0" VOIDS	MEMBRANE	
		"0" VOIDS	20% VOIDS		"0" VOIDS	20% VOIDS		"0" VOIDS	20% VOIDS
G_{11}, 10^6 PSI	10.2	10.7	8.86	15.1	11.1	8.62	13.9	15.1	11.4
G_{12}, 10^6 PSI	3.21	5.28	4.34	1.53	2.86	2.35	2.02	4.36	3.65
G_{13}, 10^6 PSI	-.17	-.75	-.81	.09	.05	-.08	~0	-.28	-.56
G_{22}, 10^6 PSI	4.01	6.24	5.26	2.49	3.68	3.05	2.93	5.47	4.51
G_{23}, 10^6 PSI	-.24	-.59	-.51	.1	-.03	-.05	-.11	-.36	-.34
G_{33}, 10^6 PSI	3.78	6.09	5.06	1.96	3.39	2.81	2.50	5.13	4.30
α_{11}, 10^{-6} IN./IN./^{0}F	-.36	-.36	-.42	-.41	-.41	-.46	-.44	-.44	-.55
α_{22}, 10^{-6} IN./IN./^{0}F	7.46	7.46	7.75	13.8	13.8	14.0	11.0	11.0	11.2
α_{12}, 10^{-6} IN./IN./^{0}F	.84	.84	.96	-.16	-.16	.02	.57	.57	.75
ρ, 10^{-4} LB-SEC^2/CM^2	1.45	1.45	1.45	1.45	1.45	1.45	1.45	1.45	1.45

CS-70182

TABLE 4.
SUMMARY OF TIP DEFLECTIONS FOR 2200 FT/SEC TIP-SPEED FIBER COMPOSITE BLADE

PROPERTIES USED	TIP DEFLECTIONS, IN.						Y-COORD DIFFER $Y_{L.E.} - Y_{T.E.}$	X-COORD DIFFER $X_{L.E.} - X_{T.E.}$	Z-COORD DIFFER $Z_{L.E.} - Z_{T.T.}$
	Y-COORD		X-COORD		Z-COORD				
	L.E.	T.E.	L.E.	T.E.	L.E.	T.E.			
BENDING STIFFNESS	0.041	0.007	0.098	0.012	-0.207	0.015	0.034	0.086	-0.222
MEMBRANE STIFFNESS	.043	.011	.085	.010	-.184	.011	.032	.075	-.195
MEMBRANE STIFFNESS 20% VOIDS & DELAMINATION NO CENTRIFUGAL STIFFENING	.051	.019	.094	-.008	-.231	.034	.032	.102	-.265
DITO WITH CENTRIFUGAL STIFFENING	.039	.024	.049	-.023	-.134	.053	.015	.072	-.187

NOTATION: FOR COORDINATE DIRECTIONS, SEE FIGURE 6.
L.E. - LEADING EDGE
T.E. - TRAILING EDGE

CS-70184

TABLE 5.
COMPUTED EFFECTS OF VARIOUS PARAMETERS
ON FREQUENCIES OF 2200 FT/SEC
FIBER COMPOSITE FAN BLADE

*ROOT FIXATION	MATERIAL	VOIDS	ROTOR SPEED	MODE FREQUENCIES, CYCLES/SEC			
				1	2	3	4
6	EQUIV MEMB STIF	0	0	361	939	1178	1485
3		0	0	327	870	1078	1387
**		0	0	337	806	1017	1191
3		20%	0	290	782	912	1258
3		20%	100	479	906	1126	1449
3	EQUIV BEND STIF	20%	100	473	832	1165	1314
3		20%	0	292	708	982	1137

CS-70166

*DEGREES OF FREEDOM (DOF) FIXED PER ROOT NODE
**SPECIAL CASE: 3-CENTER NODES 6-DOF FIXED
NODE EACH SIDE CENTER NODE 3-DOF EACH
ALL OTHERS FREE.

TABLE 6.
COMPUTED STRESSES AT REGION OF MAXIMUM
AVERAGE COMPOSITE STRESS

BLADE POINT SCHEMATIC ON FIG. 18	SURFACE STRESSES, KSI		
	RADIAL	TANGENTIAL	SHEAR
A (S. S.)	-7.86	-5.04	6.06
(P. S.)	67.1	6.21	-3.97
B	-6.18	-6.30	5.44
	64.6	7.18	-4.76
C	-4.75	-4.52	6.65
	66.0	6.31	-4.19
D	11.1	-.89	.78
	26.4	3.43	-7.40

CS-70161

NOTES: S. S. DENOTES SUCTION SURFACE.
P. S. DENOTES PRESSURE SURFACE.
CALCULATIONS ARE BASED ON EQUIVALENT BENDING STIFFNESS.
STRESSES ARE IN THE ELEMENT LOCAL COORDINATES.

TABLE 7.
COMPUTED STRESSES AT REGION OF MAXIMUM
AVERAGE COMPOSITE STRESS
"EQUIV MEMBRANE STIFFNESS" EFFECTS OF VOIDS & CENTRIFUGAL STIFFENING

BLADE POINT ON FIG. 18	SURFACE STRESSES, KSI								
	RADIAL			TANGENTIAL			SHEAR		
	*1	*2	*3	1	2	3	1	2	3
A (S. S.)	-1.93	-3.93	~0	-7.17	-8.34	-7.52	9.12	9.42	7.88
(P. S.)	58.7	61.3	57.3	11.6	12.26	11.6	-6.54	-6.02	-4.66
B	-1.70	-3.34	.57	-9.13	-10.6	-9.53	8.36	8.77	6.87
	56.5	58.3	54.3	12.3	13.3	12.5	-7.48	-7.09	-5.56
D	10.2	7.04	9.52	-2.38	-3.48	-2.53	3.30	5.03	2.68
	31.7	33.6	30.5	7.02	8.18	6.89	-13.8	-15.9	-12.9
E	12.9	11.8	13.3	2.37	4.33	2.53	4.29	5.61	3.04
	18.4	19.5	17.5	3.23	2.33	3.14	-14.8	-16.9	-13.06

*NOTES: COLUMN 1: NO VOIDS & NO CENTRIFUGAL STIFFENING
2: 20% VOIDS, 2-DELAMINATION LAYERS & NO CENTRIFUGAL STIFFENING
3: 20% VOIDS, 2-DELAMINATION LAYERS & CENTRIFUGAL STIFFENING

CS-70167

TABLE 8.
COMPUTED PLY STRESSES FOR SEVERAL LOAD CONDITIONS 2200 FT/SEC
FIBER COMPOSITE BLADE

LOADING	POINT ON FIG. 18	PLY STRESSES, KSI										INTERPLY DELAMINATION, DEGREES	
		ALONG FIBER				TRANSVERSE TO FIBER				INTRALAMINAR SHEAR			
		MINIMUM		MAXIMUM		MINIMUM		MAXIMUM		MAXIMUM		MAXIMUM	
		VALUE	PLY	VALUE	PLY	VALUE	PLY	VALUE	PLY	VALUE	PLY	VALUE	INTER-PLY
MECHANICAL	A	-25.3	1	76.7	50	-1.6	2	2.9	66	-5.03	66	0.0025	66/67
	E	-15.4	1	24.6	22	-.8	12	.6	21	3.9	22	.0018	21/22
MECHANICAL & THERMAL	A	-14.4	1	71.9	46	8.5	2	12.0	62	-4.6	62	-.0084	2/3
	E	-12.4	1	27.5	22	8.1	12	9.6	21	3.9	22	-.0069	2/3
THERMAL DUE TO FABRICATION PROCESS	A	-36.5	65	5.8	18	7.1	50	9.6	1	3.9	67	-.0055	63/64
	E	-18.2	2	7.4	12	-10.7	12	12.2	2	-2.2	21	.0031	21/22
MECHANICAL WITH CENTRIFUGAL STIFFENING (20% VOIDS)	A	-20.8	67	54.2	20	-1.6	66	3.9	2	-2.3	2	-.0036	66/67
	E	-9.1	2	61.9	1	-.9	48	4.5	2	-2.4	11	-.0050	3/2
ROOM TEMP ULTIMATE STRENGTH		-118		190		-15		4.0		6.0*		~0.0070	

CS-70185

*THIS VALUE IS APPROXIMATELY 50-PERCENT OF THE SHORT-BEAM-SHEAR (INTERLAMINAR SHEAR) STRENGTH.

FIGURE 1.

2200 FT/SEC TIP-SPEED COMPRESSOR BLADE
AS FABRICATED & TRIMMED

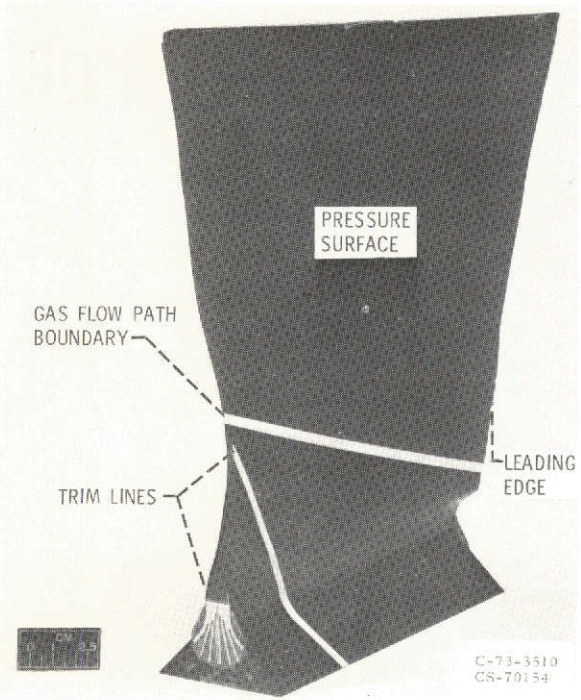

Figure 2.

2200 FT/SEC TIP-SPEED COMPRESSOR BLADE
SHOWING NONLINEAR TWIST

FIGURE 3(a).
PLY CONTOURS PRESSURE SIDE. 2200 FT/SEC TIP-SPEED FIBER COMPOSITE AIRFOIL REGION

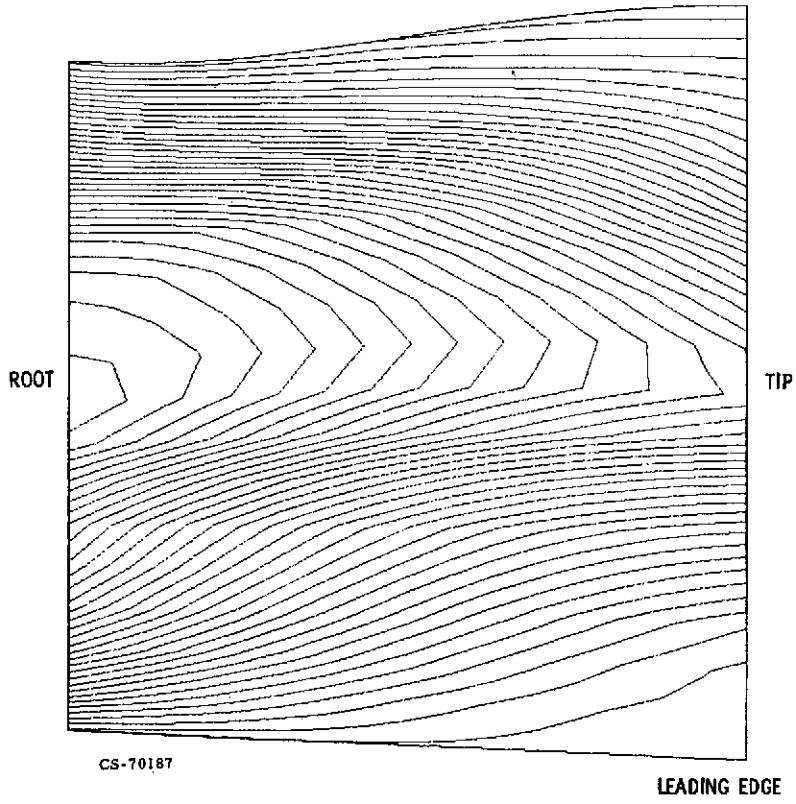

FIGURE 3(b).
PLY CONTOURS SUCTION SIDE, 2200 FT/SEC TIP-SPEED FIBER COMPOSITE AIRFOIL REGION

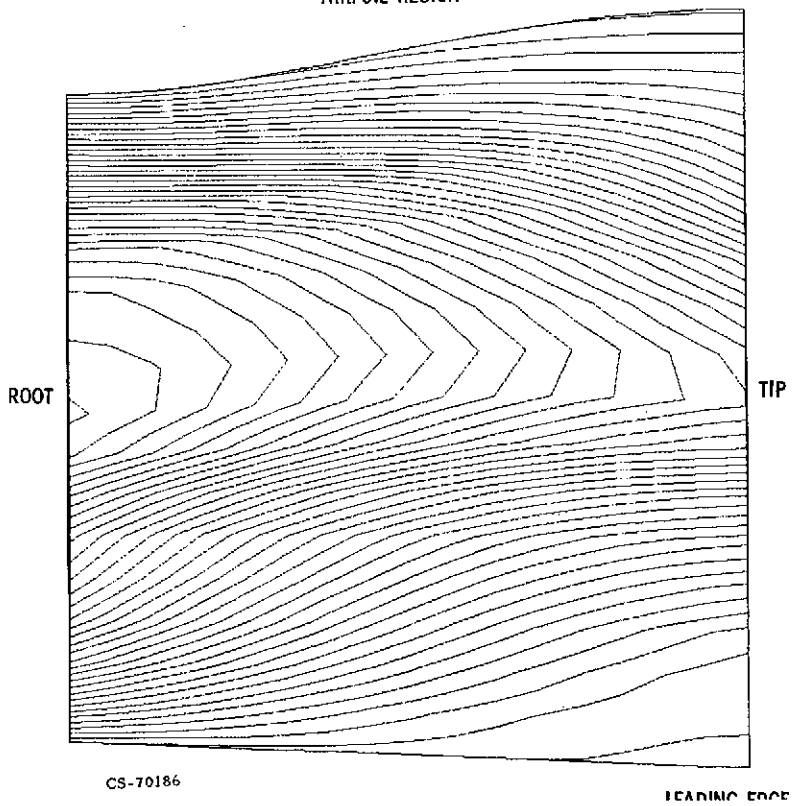

FIGURE 4.
NASTRAN FINITE ELEMENT REPRESENTATION FOR
2200 FT/SEC FIBER COMPOSITE BLADE

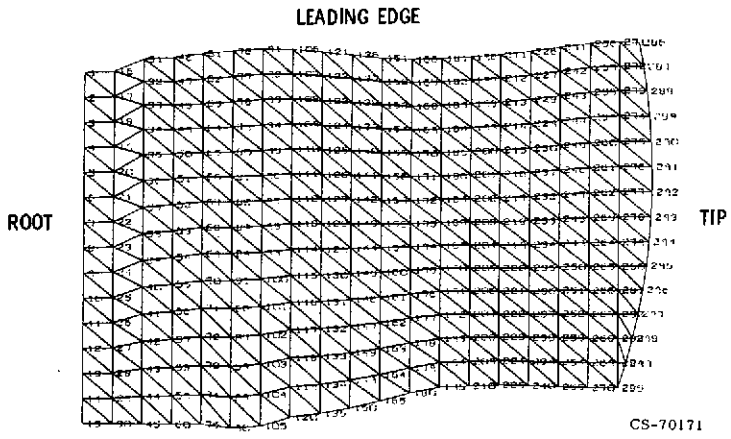

FIGURE 5.
ANALYSIS OF 2200 FT/SEC FIBER COMPOSITE BLADE USING NASTRAN

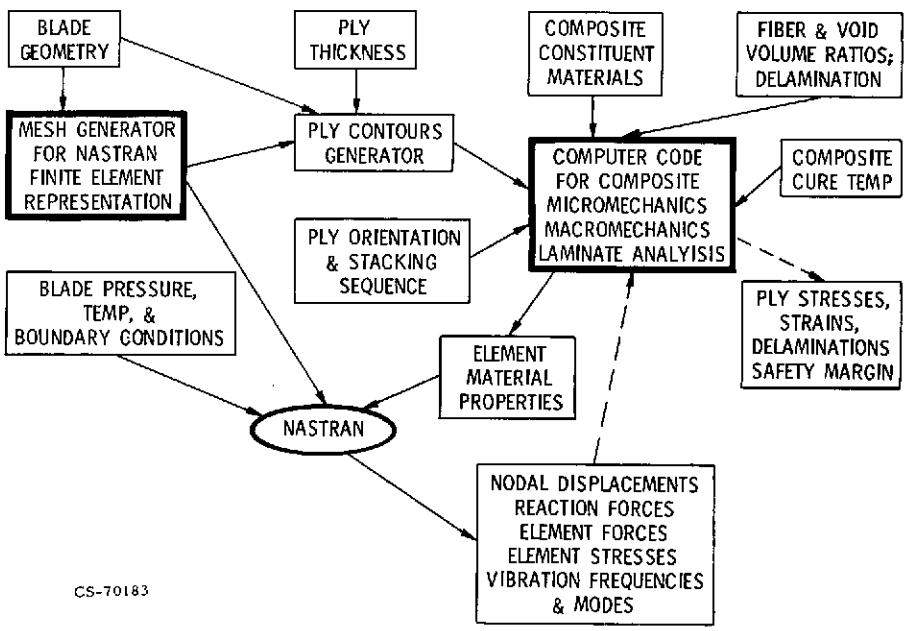

FIGURE 6.
BLADE GLOBAL COORDINATES USED FOR NASTRAN

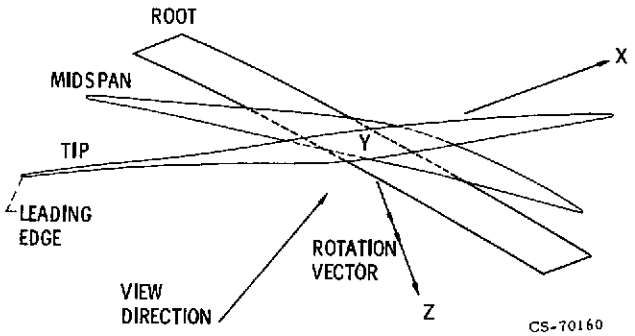

FIGURE 7.
BLADE PRESSURE CONTOURS

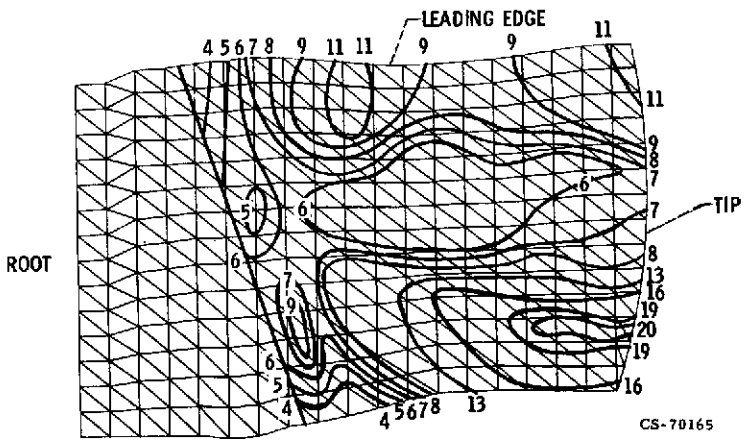

FIGURE 8.
BLADE SUBDIVISIONS FOR REPRESENTATIVE MATERIAL REGIONS

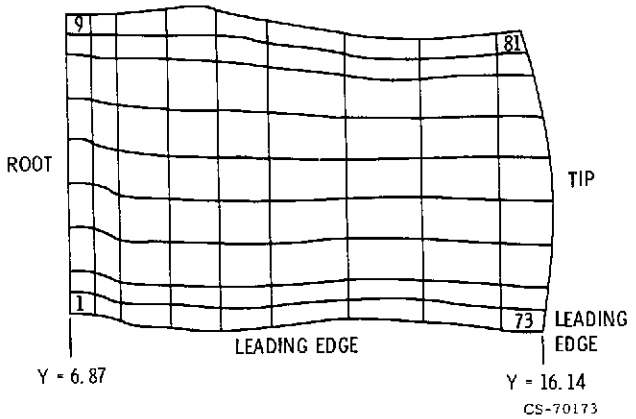

FIGURE 9.
TIP DEFLECTIONS AT 100 % DESIGN SPEED

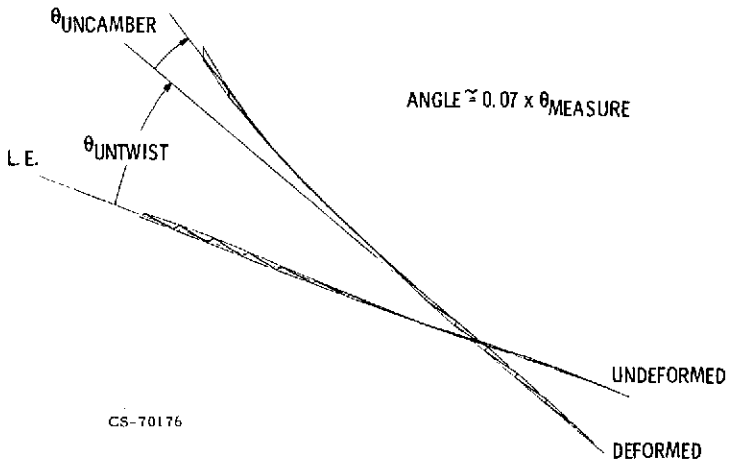

FIGURE 10.
2200 FT/SEC COMPOSITE BLADE SHAPE
AT 100% DESIGN SPEED, INCLUDING CENTRIFUGAL STIFFENING EFFECTS

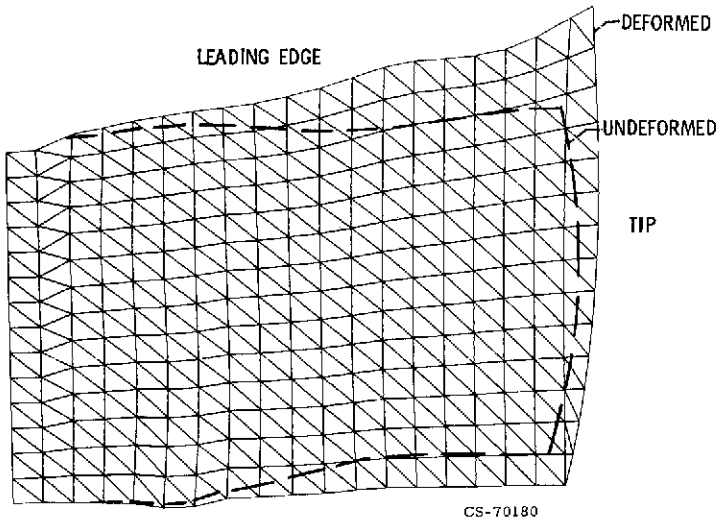

FIGURE 11.
2200 FT/SEC COMPOSITE BLADE VIBRATION
MODE NO. 1
FREQUENCY, 290 CPS

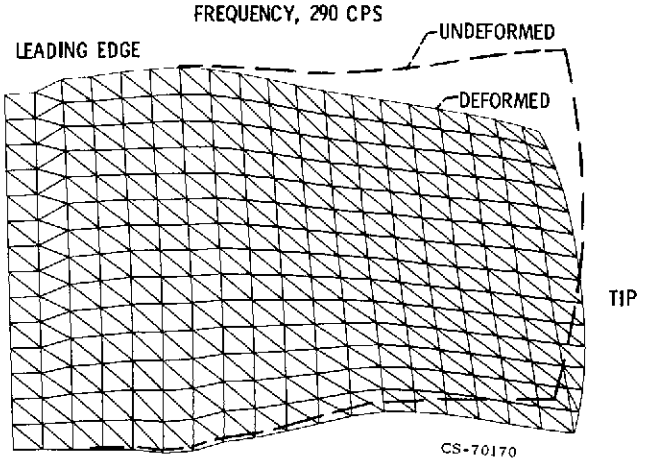

FIGURE 12.
2200 FT/SEC COMPOSITE BLADE VIBRATION
MODE NO. 2
FREQUENCY, 782 CPS

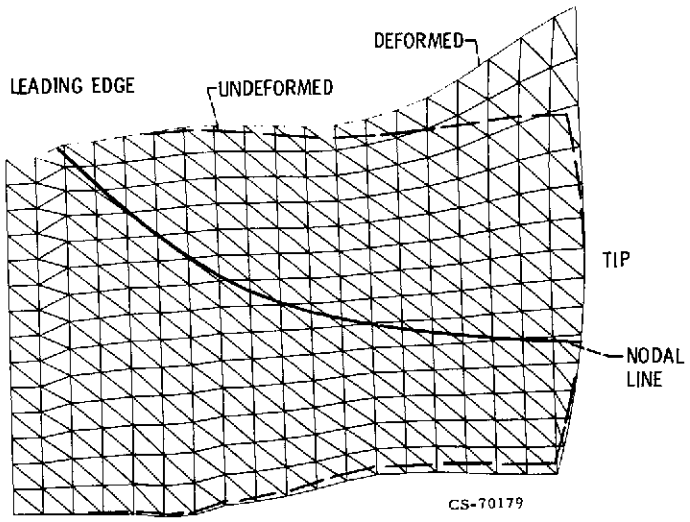

FIGURE 13.
2200 FT/SEC COMPOSITE BLADE VIBRATION
MODE NO. 3
FREQUENCY, 912 CPS

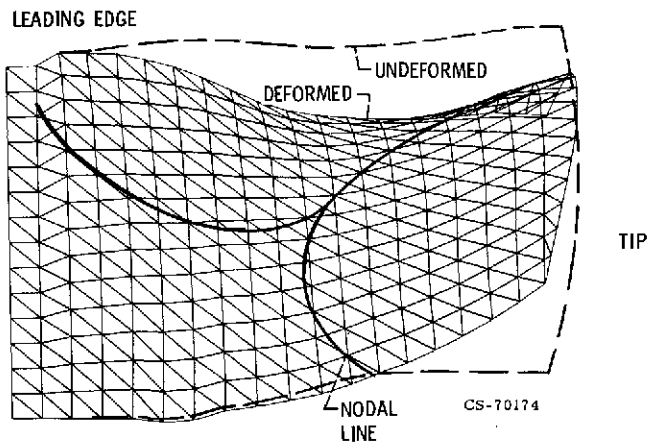

FIGURE 14.
2200 FT/SEC COMPOSITE BLADE VIBRATION
MODE NO. 4
FREQUENCY, 1258 CPS

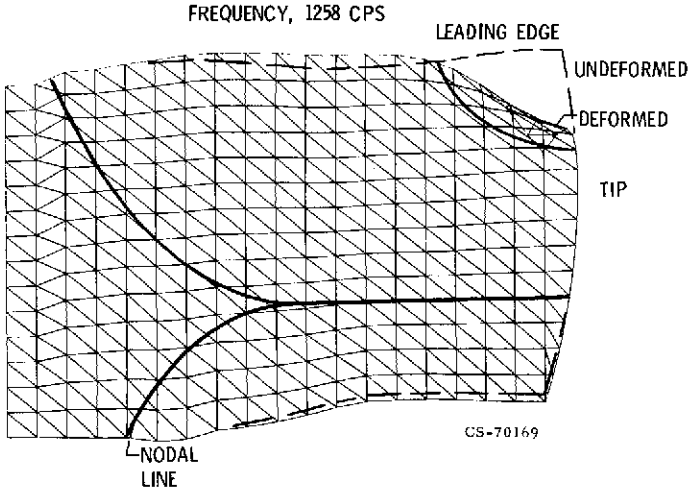

FIGURE 15.
2200 FT/SEC COMPOSITE BLADE VIBRATION
MODE NO. 5
FREQUENCY, 1825 CPS

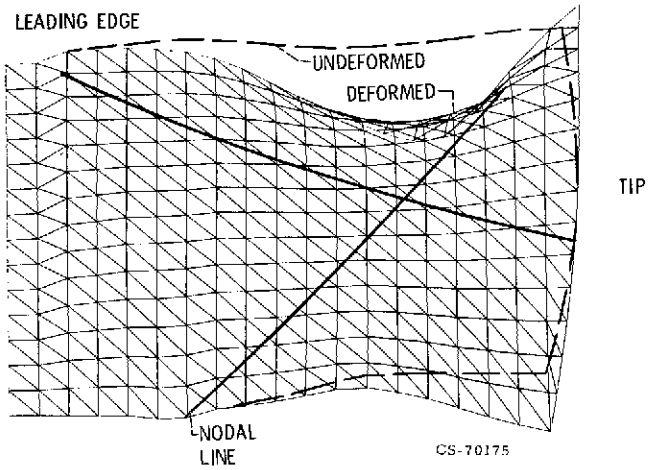

FIGURE 16.
2200 FT/SEC COMPOSITE BLADE VIBRATION
MODE NO. 6
FREQUENCY, 2011 CPS

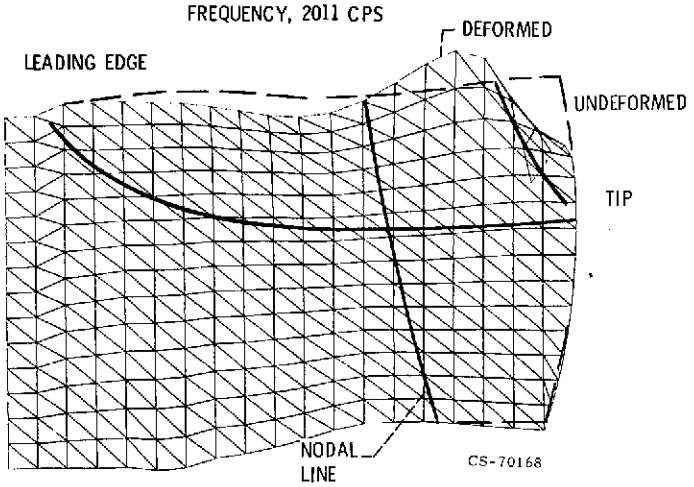

FIGURE 17.
BLADE RESONANCE FREQUENCY VS SPEED
WITH 20% VOIDS

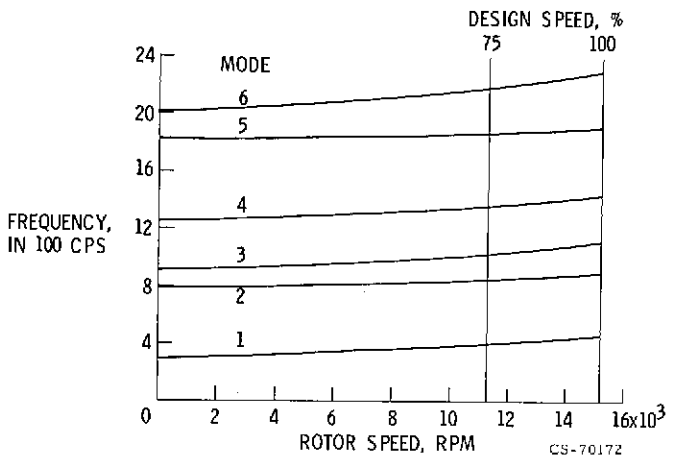

FIGURE 18.

AVERAGE COMPOSITE RADIAL STRESS CONTOURS ON PRESSURE SURFACE

EQUIVALENT BENDING STIFFNESS & NO VOIDS

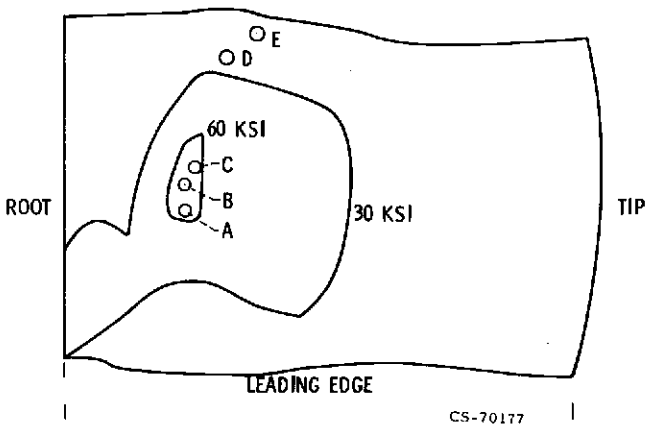

NOTES: FOR STRESS VALUES AT POINTS A, B, C, D AND E, SEE TABLES 6, 7, AND 8